sensors

MDPI

Article

V_2O_5 Thin Films as Nitrogen Dioxide Sensors †

Krystyna Schneider * and Wojciech Maziarz

AGH University of Science and Technology, Faculty of Computer Science, Electronics and Telecommunications, Department of Electronics, 30-059 Krakow, Poland; maziarz@agh.edu.pl

* Correspondence: kryschna@agh.edu.pl; Tel.: +48-12-617-2901

† This paper is an extension version of the conference paper: Krystyna Schneider and Wojciech Maziarz. Vanadium Pentoxide Thin Films: Synthesis, Characterization and Nitrogen Dioxide Sensing Properties. In Proceedings of the EUROSENSORS 2018, Graz, Austria, 9–12 September 2018.

Received: 5 October 2018; Accepted: 16 November 2018; Published: 28 November 2018

Abstract: Vanadium pentoxide thin films were deposited onto insulating support by means of rf reactive sputtering from a metallic vanadium target. Argon-oxygen gas mixtures of different compositions controlled by the flow rates were used for sputtering. X-ray diffraction at glancing incidence (GIXD) and Scanning Electronic Microscopy (SEM) were used for structural and phase characterization. Thickness of the films was determined by the profilometry. It has been confirmed by GIXD that the deposited films are composed of V_2O_5 phase. The gas sensing properties of V_2O_5 thin films were investigated at temperatures from range 410–617 K upon NO_2 gas of 4–20 ppm. The investigated material exhibited good response and reversibility towards nitrogen dioxide. The effect of metal-insulator transition (MIT) on sensor performance has been observed and discussed for the first time. It was found that a considerable increase of the sensor sensitivity occured above 545 K, which is related to postulated metal-insulator transition.

Keywords: vanadium pentoxide; thin film; reactive sputtering; electrical properties; nitrogen dioxide; gas sensor; metal-insulator transition (MIT)

1. Introduction

Increasing environmental pollution is becoming a vital global concern, particularly in relation to the imperative to reduce emissions of gases causing the greenhouse effect, acid rain, and the depletion of stratospheric ozone. Therefore, there is an urgent need to develop some devices that allow fast, portable, low-cost monitoring of the gases responsible for air pollution and/or pose danger to human health. So far, sophisticated and expensive equipment, such as gas analyzers based on IR and UV spectrophotometry, pulse fluorescence, flame photometry and gas chromatography, to determine air quality were applied. Although this equipment enables very precise gas phase analysis, it has four substantial disadvantages such as high cost, large dimensions (limited portability), slow analysis time and non-continuous monitoring of the gas composition. In this respect, chemical gas sensors may offer advantages in the form of simple construction, low cost and ability to work in situ. One large group of sensors, applied to environmental monitoring, is based on liquid (or wet) electrochemistry. However, these sensors presently suffer from the same four severe disadvantages. Moreover, these sensors cannot be applied in environments warmer than room temperature.

During the past five decades, efforts were made to develop chemical gas sensors based on solid-state technology. The potential advantages of these sensors over the wet technology sensors are (i) miniaturization, (ii) simple calibration and measurement, (iii) low cost, (iv) short response time, (v) resistance to severe conditions, such as high temperature and corrosive environment and (vi) selectivity. Their main advantage is that they can also operate at elevated temperatures, thus meeting the environmental requirements, such as for instance in car and industrial exhaust systems.

There are several types of chemical gas sensors [1]. The largest group consists of electrochemical sensors. According to Wilson et al. [2] and Janata [3] the electrochemical gas sensors have been categorized into three groups: (1) conductometric (measurement of electrical conductivity or related value such as resistivity, impedance); (2) potentiometric (measurement of electromotive force or related value such as voltage of the solid cells); (3) amperometric (measurement of current).

The most widely studied type of the gas sensors are conductometric. Their principle of operation involves a change in the resistance of the sensor sensitive phase (usually metal oxide) upon exposure to a specific component of the gas atmosphere. During adsorption of gas molecules on solid surface, the electronic charges (electrons or electron holes) are created, which change surface electrical conductivity. This process takes place within the thin layer near-surface of the solid of the thickness named the Debye length. Consequently, electrical conductivity may be used as a sensing property for detection of specific gas phase components. Various review works have referred to conductometric gas sensors [4–9]. However, there is no simple theory which can predict how the sensor's signal depends on gas concentration.

Conductometric gas sensors are usually based on metal oxide semiconductors, such as SnO_2 [10–15], ZnO [16,17], WO_3 [18], TiO_2 [19–21], Fe_2O_3 [22]. Also, other materials such as graphene, metal hydroxides, metal dichalcogenides, phosphorene, boron nitride [4,5,7], and conducting polymers are investigated. However, the poor sensor recovery and stability remain the major concerns.

Generally, semiconductor gas sensors suffer from low selectivity. Several attempts were made to improve their selectivity in respect to the detectable gas. The most frequent approach involves change of the sensor composition by doping, the use of composites with one or more other materials, variation of operating temperature etc. It was found that the successful method improving sensors' selectivity is addition of some heterogeneous catalysts, such as noble metals (Pt, Pd, Au) to the sensor material. In addition, use of the vanadium pentoxide – well-known catalyst – is promising.

Recently, vanadium oxides have attracted considerable interest due to their multi-valence, good chemical stability and excellent catalytic properties [23]. Moreover, unlike the above- mentioned sensing oxides, vanadium oxides show metal-insulator transition (MIT), an interesting electrical property which may have impact on the sensor's performance.

V_2O_5, the most stable compound among over 15 known vanadium oxides, is a promising NO_2 sensor material [24]. It demonstrated high sensitivity and selectivity for ethanol [25], ammonia [26], hydrogen and hydrocarbons [27].

Table 1 [27–49] includes examples of conductometric sensors of various gases, except of NO_2, with V_2O_5 sensing material or V_2O_5 as addition to other material such as SnO_2 [33,38], TiO_2 [40,50] and other [29,37,51–54]. On the other hand, Table 2 summarizes V_2O_5-based NO_2 sensors.

Table 1. Vanadium oxide-based gas sensors, literature survey (published between 2010–2017).

Gas	Composition	Morphology	Operation Temp (K)	Response	Gas Concentration [ppm]	Sensitive Against	Ref.
H_2 CH_4 C_3H_8	V_2O_5	Thin films	420–520	1.22	5–300 H_2 50–3000 CH_4, C_3H_8	NA	[27]
Et[1], NH_3	V_2O_5	Hollow spheres	NA[2]	Et:1.02–1.06 NH_3:1.01–1.02	100–500	NA	[28]
NH_3	V_2O_5	Thin film	RT	Change of color	100–400	H_2	[29]
Et NH_3	V_2O_5	Thin film	NA	1.04 1.06	100–500 100–500	NA NA	[30]
Acetone, CH_3OH, HCHO, toluene	VO_2	nanorods	RT[3]	1.015 1.027 1.060 1.055	5–100	NA	[31,32]
SO_2	SnO_2 + 5 wt% MgO + 2 wt% V_2O_5	Thick film	NA	1.44	0.1–1	NA	[33]
Et	V_2O_5	Thin film	508	NA	2500	NA	[34]
xylene	V_2O_5	Thin film	300	17 27.9	800 100	NH_3, Et, toluene, acetone	[35]
1-butyl-amine	V_2O_5	Nanofibres	RT	1.42	0.15–9.5	NH_3, propranolol, toluene	[36]
NH_3	V_2O_5	Composite fibers with polyvinyl acetate and pyrrolidone	530	1.02 1.06	0.1–0.8		[37]
BTEX[4]	SnO_2/V_2O_5	Composite SnO_2/V_2O_5	540	5.5–6	0.5–50	Et, CH_3OH, HCHO	[38]
CH_4	VO_2	Thin films	298–473	1.008–1.032	50–500	NO_2, H_2	[39]
NH_3	VWT: V_2O_5–WO_3–TiO_2	Potentio- metric: Au V_2O_5–WO_3–TiO_2	820	0–150	10–300	NA	[40]
H_2O	VO_2 (3fl) complex	Thick film 20-30µm	RT	NA	RH: 35–70%	NA	[41]
NH_3	V_2O_5–V_7O_{16}	Thin film	620	1.4	0.16–0.32	NO, CO	[42]
Et	V_2O_5	Thin films	573–773	1.27–1.80	500–3000	NA	[43]
Et	V_2O_5	Nanowiremicroyarns	600	9.09	50–1000	Higher alcohols	[44]
$C_4H_{10}S$ Tert-butyl mercaptan	V_2O_5	Thick layer (0.2 mm) from nanopowder	600	Catalumine-scence	3600–62,000	Alcohols, alde-hydes, NH_3	[45]
NO_x , H_2	V_2O_5 + VO_x	Thin film composed from nanotubes	448 563	2.85 1.075	20–80 NO 500–2000 H_2	CO	[46,47]
CH_4	Au–VO_x	Porous thin film	RT	NA	1500	NA	[48]
CH_4	C/VO_x	C nanotubes filled with VO_x	RT	1.015	NA	NA	[49]

Symbols: Et[1]—ethanol (C_2H_5OH); NA[2]—not reported; RT[3]—room temperature (298 K); BTEX[4]—benzene, toluene, ethylbenzene and xylene.

For some practical applications, the high operating temperature creates problems with the long-term stability and high costs of the sensor manufacture and maintenance. As can be seen in the Table 1, some authors reported that their sensors based on nanostructured vanadium pentoxide or its composite show sensitivity at room temperature [29,31,36,41,48,49]. Moreover, as per published results [40], the sensor selectivity may be substantially improved for sensors composed of oriented nanoparticles.

In this paper, the application of V_2O_5 thin films as NO_2 gas sensor is reported. The effect of MIT on sensor performance was studied for the first time.

Nitrogen dioxide, NO_2 is an extremely toxic gas. It is produced by all combustion in air and by industrial processes. NO_2 is responsible for various pollution problems such as smog and acid rain. Therefore, there is an urgent need to develop devices that allow fast, portable, low-cost monitoring of the NO_2 in the interest of environment and human health. Successful development of NO_2 gas sensors for commercialization requires the achieving of four "S", i.e. sensitivity, selectivity, stability and speed (response and recovery rates).

2. Materials and Methods

2.1. Thin Film Preparation

VO_x thin films were deposited onto insulating support (either fused silica or alumina) for sample characterization or conductometric sensor substrate type CC1.W (BVT Technologies, Czech Rep.), for electrical measurements, by means of rf sputtering in a reactive atmosphere at working pressure 4.75 Pa (24% O_2 – 76% Ar) from a metallic V target. Conductometric supports presented in Figure 1 were provided by BVT Technologies. Details of the film deposition are given elsewhere [27].

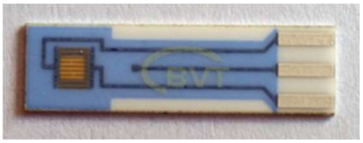

Figure 1. Conductometric sensor support from BVT Technologies company.

2.2. Morphology and Structural Characterization

Scanning electron microscopy (SEM) studies were carried out for as-sputtered thin films using NOVA NANOSEM 200 (FEI Europe Company) microscope. Phase composition of as-sputtered thin films was studied by X-ray diffraction at glancing incidence, GIXD. Thickness of the V_2O_5 thin film was (210 ± 25) nm.

2.3. Sensing Characterization

The responses S of films to the target gas (NO_2), defined as changes in electrical resistance ($S = R_{NO2}/R_{air}$), were measured by custom-made setup at different NO_2 concentrations (0–20 ppm). The sample was placed in a gas chamber on a workholder, where the temperature and gas atmosphere (gas composition and humidity) were stabilized. The relative humidity was set to 50 ± 0.1%. The requested NO_2 concentration was obtained by controlling the ratio of gas to air flow rate, and total flow rate was set to 500 cm^3/min. The total flow rate was maintained at the same level of 500 cm^3/min. The film resistance changes upon NO_2 were measured with Keithley 6517 electrometer working in constant voltage mode (U = 0.1 V). At the beginning, the sensor response has been stabilized in pre-set conditions (at the lowest temperature, constant gas flow, pure air of 50% humidity). Then two types of measurement procedures were performed. During the first stage, the measurement of sensor response under varying temperature (range 483–623 K), and at constant NO_2 concentration (20 ppm) fed alternately with air for purging purposes, was realized. After that, the second stage was performed: The measurement at constant temperature under increasing gas concentrations (0–20 ppm with 4 ppm step), also while purging the chamber with air. The sensor resistance was sampled every 2 s. The sensor measurements were performed within the temperature range extending from RT to 700 K. Equipment applied for measurements of the sensor characteristics was described in detail elsewhere [55].

3. Results and Discussion

3.1. Structural and Microstructural Characteristics

Figure 2 presents the typical XRD patterns of the sample annealed at 673 K in argon atmosphere. X-ray diffraction analysis of the samples revealed the presence of the V_2O_5 orthorhombic phase.

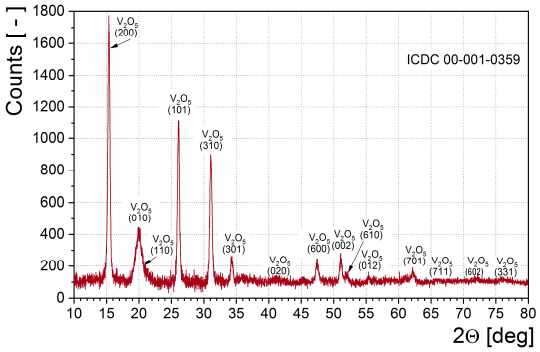

Figure 2. X-ray diffraction patterns for as-sputtered V_2O_5 thin film.

The determined lattice parameters (a = 1.145 ± 0.003 nm; b = 0.436 ± 0.004 nm; c = 0.355 ± 0.003 nm) well agree with those from literature reports [56]. Presented XRD patterns were used for determination of the crystallite size. Crystallite size, d_{XRD}, was calculated according to Scherrer's method: d_{XRD} = 20.0 ± 1.8 nm. No effect of sintering temperature on obtained XRD results was observed.

As can be seen, the as-sputtered thin films (Figure 3a) are poly-dispersed, and the grains are mostly columnar in shape with a length of 565 ± 100 nm and diameter of 220 ± 40 nm. On the other hand, after sintering (Figure 3b) they are rather spherical (mean diameter = 500 ± 75 nm). Chemical analysis performed by EDS technique revealed presence of high peaks coming from the silicon support and short peaks corresponding to oxygen and vanadium elements.

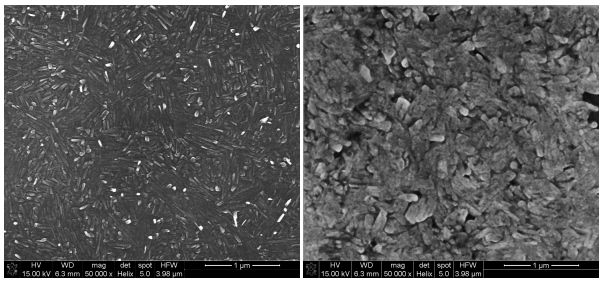

(**a**) (**b**)

Figure 3. Scanning electron micrographs of: (**a**) as-sputtered thin film; (**b**) after annealing at 673 K.

3.2. Sensing Characteristics

An example of V_2O_5 sensor responses to 20 ppm NO_2 are shown in Figure 4a,b.

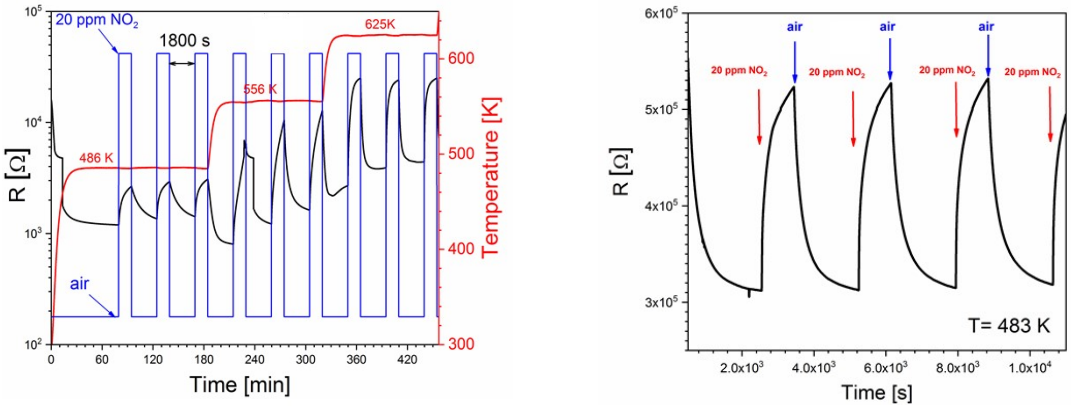

(**a**) (**b**)

Figure 4. Dynamic changes in the electrical resistance of V_2O_5 thin film upon interaction with 20 ppm NO_2, (**a**) at several temperatures; (**b**) at 483 K.

As one can see from Figure 4, the resistance of the investigated V_2O_5 thin films increases upon exposure to NO_2, which is characteristic of n-type semiconductors.

NO_2 sensing mechanism can be explained in terms of defect structure of vanadium pentoxide [57]. V_2O_5 equilibrated in air shows deficit, x, of oxygen (V_2O_{5-x}). Doubly positive ionized oxygen vacancies are compensated by V^{4+} ions. Electrical conductivity is achieved by small polaron mechanism, via electron hopping from neighbouring two ions V^{4+} and V^{5+} (marked as 1 and 2):

$$V^{4+}{}_{(1)} + V^{5+}{}_{(2)} \rightarrow V^{5+}{}_{(1)} + V^{4+}{}_{(2)} \quad (1)$$

Electrical conductivity is proportional to concentration of V^{4+} ions.

When NO_2 is added to gas atmosphere, adsorption of NO_2 molecules takes place according to the reaction:

$$\mathbf{NO_{2(g)}} + \mathbf{V^{4+}} \Rightarrow \mathbf{NO^{-}_{2(ad)}} + \mathbf{V^{5+}} \quad (2)$$

Equation (2) indicates that the increase of the resistance upon exposure of NO_2, as observed in Figure 4a,b, results from decrease of the concentration of V^{4+} ions.

Figure 5a illustrates sensor response, $S = R_{NO2}/R_{air}$, versus temperature. The abrupt increase in the sensor response is observed at 545–547 K. This behaviour may be explained by the occurrence of the metal-insulator transition, MIT.

One of the most spectacular phenomena occurring in most vanadium oxides is the abrupt change of the electrical resistivity from the values typical for semiconductor to those typical of metal phase. This phenomenon, called semiconductor–metal phase transition, SMPT [58] or more frequently metal-insulator transition, MIT, offers immense prospects for various practical applications, in particular oxide electronics, photoelectronics [59,60] and gas sensors. Strelcov et al. [61] studied gas sensor properties of nanowire VO_2 close to temperature of MIT (T_{MIT} = 338 K). They observed that varying the temperature of the nanowire close to the T_{MIT}, the conductance of the nanowire becomes extremely responsive to the tiny changes in the ambient gas environment. According to our knowledge, the effect of MIT on gas sensor properties of V_2O_5 have not been studied yet.

The single valence vanadium oxides V_2O_3, VO_2, and most of double valence vanadium oxides (i.e., Magneli or Wedsley series) show metal-insulator transition. During this transition, the polymorphic phase transition occurs from lower to higher symmetrical crystallographic structure. However, vanadium pentoxide, V_2O_5 thin film is an exception. At temperatures close to 540 K (T_{MIT} = 530 ± 5 K, Blum [59]; T_{MIT} = 553 K, Kang et al. [60]), MIT takes place in nanostructured and thin films of V_2O_5 without any phase transition. This fact can be explained that MIT in V_2O_5 is limited to the surface layer [59]. Our recent studies revealed that MIT is observed in V_2O_5 thin films annealed in air, while in V_2O_5 thin films annealed in gas atmosphere containing NO_2 MIT effect was not observed. From these facts and Equation (2), we postulate that sufficient V^{4+} ion concentration on the surface is a prerequisite to MIT in vanadium pentoxide. The abrupt change (Figure 5a) of sensor response S, which is observed close to T_{MIT}, results from MIT in sample in air (i.e. abrupt decrease of R_{air}, and much smaller increase in R_{NO2}.

As Figure 5b indicates, below T_{MIT} ($T < T_{MIT}$ = 546 K), the sensor response S increases slightly with temperature. On the other hand, for $T > T_{MIT}$ the sensor response exhibits much larger increase.

Table 2. Vanadium oxide-based semiconducting NO_2 sensors.

Materials	Operation Temperature [K]	Concentration	Response	Reference
VO_2 thin film nanocolumnar	423	>100 ppm	5	[24]
V_2O_5 thin film nanotubes	563	20–80 ppm	6	[47]
V_2O_5 thin film nanotubes	448	20–80 ppm	2.9	[47]
Composite porous Si/ nanorods V_2O_5	298–523	0.25–3	5–10	[51]
V_2O_5 thin film	553–573	100 ppm	1.6	[62]
V_2O_5 thin films composed from-nanorods	473	100 ppm	1.24	[63]
V_2O_5 thin films 450 nm	323	2–20 ppm	1.8	[64]
V_2O_5 nanorods	473	100 ppm	1.75 1.24	[65] [66]
V_2O_5 thin films	410–545	4 ppm 20 ppm	1.16 3.35	This work
V_2O_5 thin films	546–617	4 ppm 20 ppm	14.4 23.0	This work

Some examples of NO_2 sensor with vanadium pentoxide sensing material are given in Table 2 [47,62–65]. Among gas sensing oxides presented in Table 2, two materials distinguish oneself: composite porous Si/nanorod V_2O_5 [51] and thin film V_2O_5 (this work) sensors. They enabled detection of low NO_2 concentrations below 5 ppm. They showed the highest response S = 5–10 [51] and S = 14–23 (this work), respectively. Proposed by Yan et al. [51] sensor can work at room temperature. However, the instability of gas sensitivity, lack thermal stability of porous silicon [66], as well as complex technology of manufacturing of the porous Si/nanorod V_2O_5 composite [51] limit the commercial applications.

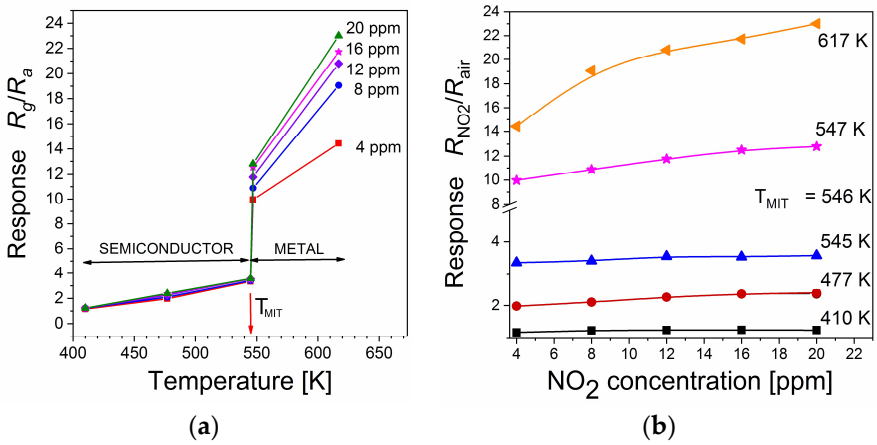

Figure 5. The sensor response S: (**a**) *vs.* temperature for various NO_2 concentrations and (**b**) *vs.* NO_2 concentration for different temperatures.

4. Conclusions

In the present work, we fabricated V_2O_5 thin films by rf reactive sputtering. The film structure and morphology were studied by X-ray diffraction at glancing incidence and scanning electronic microscopy. Gas sensing studies showed that the V_2O_5 thin films were sensitive to NO_2 at relatively low operating temperatures. The considerable increase of the sensor sensitivity was observed above 545 K, which is related to postulated metal-insulator transition. Presented studies on vanadium pentoxide thin film NO_2 sensor will be continued regarding selectivity (especially in respect to water vapor).

Author Contributions: Conceptualization, K.S. and W.M.; Methodology, K.S. and W.M.; Investigation, K.S. and W.M.; Writing—Original Draft, K.S. and W.M.; Writing—Review & Editing, K.S. and W.M.; Funding Acquisition, K.S. and W.M.; Resources, K.S. and W.M.; Supervision, K.S. and W.M.

Acknowledgments: This work was financially supported by the National Science Centre of the Republic of Poland, under Grant No. 2016/23/B/ST8/00163.

Conflicts of Interest: The authors declare no conflict of interest.

References

1. Xu, K.; Fu, C.; Gao, Z.; Wei, F.; Yiang, Y.; Xu, C. Nanomaterials-based gas sensor: A review. *J. Instr. Sci. Technol.* **2018**, *46*, 115–145. [CrossRef]
2. Wilson, L.G.; Everett, L.G.; Cullen, S.J. *Handbook of Vadose Zone Characterization Monitoring*; CRC Press: Boca Raton, FL, USA, 1995.
3. Janata, J. Potentiometric microsensors. *Chem. Rev.* **1990**, *5*, 691–703. [CrossRef]
4. Liu, X.; Ma, T.; Pinna, N.; Zhang, J. Two-dimensional nanostructured materials for gas sensing. *Adv. Funct. Mater.* **2017**, *27*, 1702168. [CrossRef]
5. Moseley, P.T. Progress in the development of semiconducting metal oxide gas sensors: A review. *Meas. Sci. Technol.* **2017**, *28*, 082001. [CrossRef]
6. Zhang, J.; Liu, X.; Neri, G.; Pinna, N. Nanostructured materials for room-temperature gas sensors. *Adv. Mater.* **2016**, *28*, 795–811. [CrossRef] [PubMed]
7. Joshi, N.; Hayasaka, T.; Liu, Y.; Liu, H.; Oliveira, O.N.; Lin, L. A review on chemiresistive room temperature gas sensors based on metal oxide nanostructured, graphene and 2D metal dichalcogenides. *Microchim. Acta* **2018**, *185*, 213. [CrossRef] [PubMed]
8. Yang, S.; Jiang, C.; Wei, S. Gas sensing in 2D materials. *Appl. Phys. Rev.* **2017**, *2*, 021304. [CrossRef]
9. Bishnoi, A.; Kumar, S.; Joshi, N. Wide-Angle X-ray Diffraction (XRD): Technique for Characterization of Nanomaterials and Polymer Nanocomposites. In *Microscopy Methods in Nanomaterials Characterization*; Sabu, T., Raju, T., Ajesh, Z., Raghvendra, M., Eds.; Elsevier: Amsterdam, The Netherlands, 2017; pp. 313–337.
10. Szklarski, Z.; Zakrzewska, K.; Rekas, M. Tin oxide films as gas sensors. *Thin Solid Films* **1989**, *174*, 269–275. [CrossRef]
11. Yamazoe, N. New approaches for improving semiconductor gas sensors. *Sens. Actuators B* **1991**, *5*, 7–19. [CrossRef]
12. Teterycz, H.; Kita, J.; Bauer, R.; Golonka, L.J.; Licznerski, B.W.; Nitsch, K.; Wisniewski, K. New design of SnO_2 gas sensor on low temperature cofiring ceramics. *Sens. Actuators B* **1998**, *47*, 100–103. [CrossRef]
13. Zeng, W.; Liu, T.; Liu, D.; Han, E. Hydrogen sensing and mechanism of doped SnO_2 (M = Cr^{3+}, Cu^{2+} and Pd^{2+}) nanocomposite. *Sens. Actuators B* **2011**, *160*, 455–462. [CrossRef]
14. Gyu, C.N.; Jin, Y.D.; Mi-Jin, J.; Ho-Gi, K.; Tuller, H.L.; Il-Doo, K. Highly sensitive SnO_2 hollow nanofiber-based NO_2 gas sensor. *Sens. Actuators B* **2011**, *160*, 1468–1470.
15. Jeun, J.H.; Kim, D.H.; Hong, S.H. Synthesis of porous SnO_2 foams on SiO_2/Si substrate by electrochemical deposition and their gas sensing properties. *Sens. Actuators B* **2012**, *161*, 784–790. [CrossRef]
16. Liu, Y.; Hang, T.; Xie, Y.; Bao, Z.; Song, J.; Zhang, H.; Xie, E. Effect of Mg doping on the hydrogen-sensing characteristics of ZnO thin films. *Sens. Actuators B* **2011**, *160*, 266–270. [CrossRef]
17. Hassan, K.; Chung, G. Catalytically activated quantum size Pt/Pd bimetallic core-shell nanoparticles decorated on ZnO nanorod clusters for accelerated hydrogen gas detection. *Sens. Actuators B* **2017**, *239*, 824–833. [CrossRef]
18. Perfecto, T.M.; Zito, C.A.; Volanti, D.P. Design of nanostructured $WO_3 \cdot 0.33H_2O$ via combination of ultrasonic spray nozzle and microwave-assisted hydrothermal methods for enhancing isopropanol gas sensing at room temperature. *Cryst. Eng. Comm.* **2017**, *19*, 2733–2738. [CrossRef]
19. Zakrzewska, K.; Radecka, M.; Rekas, M. Effect of Nb, Cr, Sn additions on gas sensing properties of TiO_2 thin films. *Thin Solid Films* **1997**, *310*, 161–166. [CrossRef]
20. Li, Y.; Wlodarski, W.; Galatsis, K.; Moslih, S.H.; Cole, J.; Russo, S.; Rockelman, N. Gas sensing properties of p-type semiconducting Cr-doped TiO_2 thin films. *Sens. Actuators B* **2002**, *83*, 160–163. [CrossRef]

21. Lyson-Sypien, B.; Czapla, A.; Lubecka, M.; Gwizdz, P.; Schneider, K.; Zakrzewska, K.; Michalow, K.; Graule, T.; Reszka, A.; Rekas, M.; et al. Nanopowders of chromium doped TiO_2 for gas sensors. *Sens. Actuators B* **2012**, *175*, 163–172. [CrossRef]
22. Flak, D.; Braun, A.; Michalow, K.A.; Parlinska-Wojtan, J.W.M.; Graule, T.; Rekas, M. Differences in electrophysical and gas sensing properties of flame spray synthesized Fe_2O_3 (γ-Fe_2O_3 and α-Fe_2O_3). *J. Nanosci. Nanotechnol.* **2012**, *12*, 6401–6411. [CrossRef] [PubMed]
23. Beke, S. A review of the growth of V_2O_5 films from 1885 to 2010. *Thin Solid Films* **2011**, *519*, 1761–1771. [CrossRef]
24. Han, S.D.; Moon, H.G.; Noh, M.S.; Pyeon, J.J.; Shim, Y.S.; Nahm, S.; Kim, J.S.; Yoo, K.S.; Kang, C.Y. Self-doped nanocolumnar vanadium oxides thin films for highly selective NO_2 gas sensing at low temperatures. *Sens. Actuators B* **2017**, *241*, 40–47. [CrossRef]
25. Liu, J.; Wang, X.; Peng, Q.; Li, Y. Vanadium pentoxide nanobelts: Highly selective and stable ethanol sensor material. *Adv. Mater.* **2005**, *17*, 764–767. [CrossRef]
26. Huotari, J.; Bjorklund, R.; Lappalainen, J.; Spetz, L.A. Nanostructured mixed phase vanadium oxide thin films as highly sensitive ammonia sensing material. *Procedia Eng.* **2014**, *87*, 1035–1038. [CrossRef]
27. Schneider, K.; Lubecka, M.; Czapla, A. V_2O_5 thin films for gas sensor applications. *Sens. Actuators B* **2016**, *206*, 970–977. [CrossRef]
28. Raj, D.; Pazhanieval, T.; Kumar, P.S.; Mangalareaj, D.; Nataraj, D.; Ponpandian, N. Self-assembler V_2O_5 nanorods for gas sensors. *Current Appl. Phys.* **2010**, *10*, 531–537.
29. Rizzo, G.; Arena, A.; Bonavita, A.; Donato, N.; Neri, G.; Saitt, G. Gasochromic response of nanocrystalline vanadium pentoxide films deposited from ethanol dispersions. *Thin Solid Films* **2010**, *518*, 7124–7127. [CrossRef]
30. Raj, A.D.; Mangalaraj, D.; Ponpandian, N.; Yi, J. Gas sensing properties of chemically synthesized V_2O_5 thin films. *Adv. Mater. Res.* **2010**, *123*, 683–686.
31. Li, S.C.; Hwang, B.W.; Lee, S.J.; Choi, H.Y.; Kim, S.Y.; Jung, S.Y. A novel tin oxide-based recoverable thick film SO_2 gas sensor promoted with magnesium and vanadium oxides. *Sens. Actuators B* **2011**, *160*, 1328–1334.
32. Simo, A.; Kasviyarasu, K.; Mwakilunga, B.; Mokwena, M.; Maaza, M. Room temperature volatile organic compound gas sensor based on vanadium oxide 1-dimension nanoparticles. *Ceram. Int.* **2017**, *43*, 1347–1363. [CrossRef]
33. Izu, N.; Hagen, G.; Schönauer, D.; Röder-Roith, U.; Moos, R. Application of $V_2O_5/WO_3/TiO_2$ for resistive-type SO_2 sensors. *Sensors* **2011**, *11*, 2982–2991.
34. Khatibani, A.B.; Abbasi, M.; Rozati, S.M. Pecularities of deposition times on gas sensing behaviour of vanadium oxide thin films. *Acta Phys. Pol. A* **2016**, *129*, 1245–1251. [CrossRef]
35. Vijayakumar, Y.; Mani, G.K.; Reddy, M.R.; Rayappan, J.B.B. Nanostructured flower like V_2O_5 thin films and its room temperature sensing characteristics. *Ceram. Int.* **2015**, *41*, 2221–2227. [CrossRef]
36. Raible, I.; Burghard, M.; Schlecht, U.; Yasuda, A.; Vossmeyer, T. V_2O_5 nanofibres: Novel gas sensors with extremely high sensitivity and selectivity to amines. *Sens. Actuators B* **2005**, *106*, 730–735.
37. Modafferi, V.; Trocino, S.; Donato, A.; Panzera, G.; Neri, G. Electrospun V_2O_5 composite fibers: Synthesis, characterization and ammonia sensing properties. *Thin Solid Films* **2013**, *548*, 689–694. [CrossRef]
38. Zhang, F.; Wang, X.; Dong, J.; Qin, N.; Xu, J. Selective BTEX sensor based on SnO_2/V_2O_5 composite. *Sens. Actuators B* **2013**, *186*, 126–131. [CrossRef]
39. Prasad, A.K.; Amirthapandiana, S.; Dharaa, S.; Dasha, S.; Muralib, N.; Tyagia, A.K. Novel single phase vanadium dioxide nanostructured films for methane sensing near room temperature. *Sens. Actuators B* **2014**, *191*, 252–256. [CrossRef]
40. Schönauer-Kamin, D.; Fleischer, M.; Moos, R. Influence of the V_2O_5 content of the catalyst layer of a non-Nerstian NH_3 sensor. *Solid State Ion.* **2014**, *262*, 270–273.
41. Karimov, K.S.; Saleem, M.; Mahroof-Tahir, M.; Akram, R.; Chanee, M.T.S.; Niaz, A.K. Resistive humidity sensor based on vanadium complex films. *J. Semicond.* **2014**, *9*, 094001. [CrossRef]
42. Huotari, J.; Bjorklund, R.; Lappalainen, J.; Spetz, A.L. Pulsed laser deposited nanostructured vanadium oxide thin films characterized as ammonia sensors. *Sens. Actuators B* **2015**, *217*, 22–29. [CrossRef]

43. Abbasi, M.; Rozati, S.M.; Irani, R.; Beke, S. Synthesis and gas sensing behaviour of nanostructured V_2O_5 thin films prepared by spray pyrolysis. *Mater. Sci. Semicond. Process* **2015**, *29*, 132–138. [CrossRef]
44. Jin, W.; Yan, S.; An, L.; Chenb, W.; Yang, S.; Zhao, C.; Dai, Y. Enhancement of ethanol gas sensing response based on ordered V_2O_5 nanowire microyarns. *Sens. Actuators B* **2015**, *206*, 284–290. [CrossRef]
45. Zhang, H.; Zhang, L.; Hu, J.; Cai, P.; Lv, Y. A cataluminescence gas sensor based on nanosized V_2O_5 for tert-butyl merkaptan. *Sens. Actuators B* **2015**, *206*, 284–290.
46. Tolhurst, T.M.; Leedahl, B.; Andrews, J.L.; Banerjee, S.; Moewes, A. The electronic structure of ε'-V_2O_5: An expanded band gap in a double-layered polymorph with increased interlayer separation. *J. Mater. Chem. A* **2017**, *45*, 23694–23703. [CrossRef]
47. Huotari, J.; Lappalainen, J.; Puustinen, J.; Spetz, A.L. Gas sensing properties of pulsed laser deposited vanadium oxide thin films with various crystal structures. *Sens. Actuators B* **2013**, *187*, 386–394. [CrossRef]
48. Liang, J.; Liu, J.; Li, W. Magnetron sputtered Au-decorated vanadium oxides composite thin films for methane-sensing properties at room temperature. *J. Alloys Compounds* **2016**, *671*, 283–290. [CrossRef]
49. Chimowa, G.; Tshabalala, Z.P.; Akande, A.A.; Bepete, G.; Mwakikunga, B.; Ray, S.S.; Banecha, E.M. Improving methane gas sensing properties of multi-walled carbon monotubes by vanadium oxide filing. *Sens. Actuators B* **2017**, *247*, 11–18. [CrossRef]
50. Carotta, M.C.; Ferroni, M.; Gherardi, S.; Guidi, V.; Malagu, C.; Martinelli, G.; Sacerdoti, M.; di Vona, M.; Licoccia, S.; Traversa, E. Thick-film gas sensors based on vanadium–titanium oxide powders prepared by sol-gel synthesis. *J. Eur. Ceram. Soc.* **2004**, *24*, 1409–1413. [CrossRef]
51. Yan, W.; Hu, M.; Wang, D.; Li, C. Room temperature gas sensing properties of porous silicon/V_2O_5nanorods composite. *Appl. Surf. Sci.* **2015**, *346*, 216–222. [CrossRef]
52. Wang, C.; Chen, H.; Chen, Y. Gold/vanadium-tin oxide nanocomposites prepared by coprecipitation method for carbon monoxide gas sensors. *Sens. Actuators B* **2013**, *176*, 945–951. [CrossRef]
53. Jin, A.; Chen, W.; Zhu, Q.; Yang, Y.; Volkov, V.I.; Zakharova, G.S. Structural and electrochromic properties of molybdenum doped vanadium pentoxide thin films by sol-gel and hydrothermal synthesis. *Thin Solid Films* **2009**, *517*, 2023–2028. [CrossRef]
54. Yu, H.Y.; Kang, B.H.; Pi, U.H.; Park, C.W.; Choi, S.; Kim, G.T. V_2O_5 nanowire based nanoelectronic devices for helium detection. *Appl. Phys. Lett.* **2005**, *86*, 253102. [CrossRef]
55. Maziarz, W.; Kusior, A.; Trenczek-Zajac, A. Nanostructured TiO_2-based gas sensors with enhanced sensitivity to reducing gases. *Beilstein J. Nanotechnol.* **2016**, *7*, 1718–1726. [CrossRef] [PubMed]
56. Chakrabarti, A.; Hermann, K.; Druzinic, R.; Witko, M.; Wagner, F.; Petersen, M. Geometric and electronic structure of vanadium pentoxide: A density functional bulk and surface study. *Phys. Rev. B* **1999**, *59*, 10583–10590. [CrossRef]
57. Schneider, K. Defect structure of V_2O_5 thin film gas sensors. In Proceedings of the SPIE 10161, 14th International Conference on Optical and Electronic Sensors, 1016109, Gdansk, Poland, 19–22 June 2016.
58. Osmolovskaya, O.M.; Murin, I.V.; Smirnov, V.M.; Osmolovsky, M.G. Synthesis of vanadium dioxide thin films and nanoparticles: A brief review. *Rev. Adv. Mater. Sci.* **2014**, *36*, 70–74.
59. Blum, R.P.; Niehus, H.; Hucho, C.; Fortrie, R.; Ganduglia-Pirovano, M.V.; Sauer, J.; Shaikhutdinov, S.; Freund, H.J. Surface metal-insulator transition on a vanadium pentoxide (001) single crystal. *Phys. Rev. Lett.* **2007**, *99*, 226103–226104. [CrossRef] [PubMed]
60. Kang, M.; Kim, I.; Kim, S.W.; Ryu, J.W.; Park, H.Y. Metal-insulator transition without structural phase transition in V_2O_5 film. *Appl. Phys. Lett.* **2011**, *98*, 131907–131916. [CrossRef]
61. Strelcov, E.; Lilach, Y.; Kolmakov, A. Gas sensor based on metal-insulator transition in VO_2 nanowire thermistor. *Nano Lett.* **2009**, *9*, 2322–2326. [CrossRef] [PubMed]
62. Rella, R.; Siciliano, P.; Cricenti, A.; Generosi, R.; Coluzza, C. A study of physical properties and gas-surface interaction of vanadium oxide thin films. *Thin Solid Films* **1999**, *349*, 254–259. [CrossRef]
63. Mane, A.A.; Suryawanshi, M.P.; Kim, J.H.; Moholkar, A.V. Fast response of sprayed vanadium pentoxide (V_2O_5) nanorods towards nitrogen dioxide (NO_2) gas detection. *Appl. Surf. Sci.* **2017**, *403*, 540–550. [CrossRef]
64. Prasad, A.K.; Dhara, S.; Dash, S. Selective NO_2 sensor based on nanostructured vanadium oxide films. *Sensor Lett.* **2017**, *15*, 552–556. [CrossRef]

65. Mane, A.A.; Suryawanshi, M.P.; Kim, J.H.; Moholkar, A.V. Superior selectivity and enhanced response characteristics of palladium sensitized vanadium pentoxide nanorods for detection of nitrogen dioxide gas. *J. Colloid Interface Sci.* **2017**, *495*, 53–60. [CrossRef] [PubMed]
66. Kunango, J.; Saha, H.; Basu, S. Pd selenized porous silicon hydrogen sensor-influence of ZnO thin film. *Sens. Actuators B* **2010**, *147*, 128–136. [CrossRef]